

Molecular Crystals with Dimensionally Controlled Hydrogen-Bonded Nanostructures

Victoria A. Russell and Michael D. Ward*

Department of Chemical Engineering and Materials Science, University of Minnesota,
Amundson Hall, 421 Washington Ave. SE, Minneapolis, Minnesota 55455

Received February 1, 1996. Revised Manuscript Received April 16, 1996⁸

Molecular crystals constructed by hydrogen bonding can be viewed as having nanostructural elements consisting of ordered, supramolecular hydrogen-bonded networks. These networks, whose dimensionalities and motifs are governed by the molecular structure and hydrogen-bonding topology of their constituents, can serve as “modules” in the design and synthesis of molecular materials. Robust supramolecular modules can reduce significantly the number of possible solid-state packing motifs, a key goal of crystal engineering strategies which aim to design and synthesize molecular solids with controlled solid-state structure and properties. Several examples of hydrogen bonded modules in molecular crystals are described, including one-dimensional hydrogen-bonded wires, two-dimensional hydrogen-bonded layers, and nanoporous hydrogen-bonded lattices with voids having differing dimensionalities. The presence of reliable modules in these materials provides for a better general understanding of the organization principles governing molecular and solid-state assembly by reducing the number of variables in systematic studies.

Introduction

Molecular crystals, which consist of organic molecules, organometallic molecules or coordination complexes assembled in the solid state as a consequence of non-covalent interactions, have been the subject of numerous investigations during the last several decades. The interest in these materials stems from the potential to manipulate solid-state properties of single crystals by systematic variations of the molecular structure and properties of the molecular components. This was made evident by the pioneering studies of Schmidt,¹ who demonstrated that different solid-state packing arrangements (i.e., polymorphs) of cinnamic acids led to starkly different photodimerization behavior. This discovery led to the emergence of “crystal engineering” for the design and synthesis of functional materials.² The diverse variety of molecular structures available by synthetic chemistry and an understanding of structure–function relationships conspire to make crystal engineering a promising approach to new materials whose properties can be controlled at the molecular level. This can be viewed as “supramolecular synthesis”, which is analogous to molecular synthesis except that weak non-covalent bonding interactions control the structure of the solid state. This has led to numerous molecular crystals exhibiting properties normally associated with conventional elemental and inorganic solids, including nonlinear optical behavior, electrical conductivity, superconductivity, and ferromagnetism.^{3–6} Molecular-level control of solid-state structure may lead to new clathrate compounds in which functional guest molecules are trapped in nanoporous host lattices with molecular-sized voids with tailored environments (e.g., hydrophobic vs hydrophilic, polar vs nonpolar). The

soluble nature of molecular materials may provide advantages in processing of useful bulk or thin-film forms.

Central to the crystal engineering strategy is a thorough understanding, and ultimately control of, the assembly of constituent molecules into desirable supramolecular motifs in the solid state. While crystal engineering has advanced significantly since its inception, the ability to control solid-state packing is commonly thwarted by the unpredictable nature of the weak and nondirectional nature of the nonbonding interactions between molecules in the solid state. This is apparent from the ubiquitous appearance of polymorphism and pseudopolymorphism in molecular crystals,⁷ which reflects the small energetic differences between different crystal packing motifs. The selectivity toward polymorphs is governed by any of several experimental variables capable of influencing the nucleation kinetics of the different crystal forms. These variables include temperature, solvent, and the composition and structure of interfaces upon which heterogeneous nucleation occurs.⁸

The success of crystal engineering strategies hinges on identification of the key nanostructural elements of molecular crystals, the design of new crystalline phases based on these elements, and the introduction of desirable functionality. These structural elements may be single molecules held together in the solid state by weak, nondirectional van der Waals interactions or by strong directional interactions. However, these elements also can be low-dimensional, robust supramolecular aggregates which retain their integrity upon crystallization into three-dimensional lattices. Robustness is defined here as an aggregate which retains the principal characteristics of its supramolecular structure regardless of ancillary functional groups or the presence of other molecular species in the crystal lattice. Crystal design based on robust aggregates has the advantage of limiting the degrees of freedom in crystal packing

* To whom correspondence should be addressed.

⁸ Abstract published in *Advance ACS Abstracts*, July 15, 1996.

during their assembly into a three-dimensional crystal, thereby improving the predictability of crystal structures. The utility of robust networks in the design of functional materials has been demonstrated amply for inorganic networks such as zeolites, clays and metal phosphates and phosphonates. Zeolites can separate small molecules by size discrimination provided by nanoscale voids, provide novel reaction environments for small molecules,⁹ and provide lattice sites for quantum-sized particles.¹⁰ Layered clays¹¹ and metal phosphates and phosphonates^{12,13} have robust two-dimensional inorganic networks that serve to spatially isolate molecular species, leading to controlled separations and reactivity. The robustness of the two-dimensional Zr(PO₃)₂ layers has enabled the incorporation of a diverse variety of organic functionality within the layers without severe perturbation of the parent structure.

The purpose of this review is to provide illustrative examples of molecular crystals which possess robust networks with preordained motifs as a consequence of structurally directing hydrogen bonding. The nanostructural building blocks in these materials include single molecules with hydrogen-bonding functionality, or robust low-dimensional hydrogen-bonded supramolecular aggregates whose dimensionality is governed by molecular hydrogen-bonding valency and topology. Conformationally rigid molecules can form networks whose structures can be predicted qualitatively from the topology described by hydrogen-bonding substituents. The role of robust low-dimensional aggregates as reliable supramolecular "modules" which assemble into three-dimensional lattices is emphasized. These aggregates can reduce crystal engineering to one or two dimensions, thereby improving the predictability of crystal structures.

Low-Dimensional Aggregates in Crystal Engineering

Several research groups recently have recognized the important of designing molecular crystals based on low-dimensional aggregates. Much of this work stems from very early studies by Kitaigorodsky, who demonstrated that molecules will tend to crystallize into space groups that contain inversion centers or translation symmetries such as glide planes and screw axes, as these operations favor close packing.^{14,15} These concepts have been extended to describe crystal structure in terms of geometric packing of rigid organic molecules into one- and two-dimensional structures in crystalline lattices.^{16,17} The relationship between local symmetry and crystal structure was made evident by calculations involving small "nuclei" consisting of 2–4 molecules organized about common symmetry elements, followed by lattice translation to build the crystal structure.¹⁸ These calculations involved first determining the minimum energy structures of nuclei in which the molecules were related by inversion, screw or glide operations, followed by translational searches for energy minima, with the ultimate space group related to the choice of nuclei symmetry. This approach was reasonably successful in terms of reproducing experimentally observed crystal structures and was more convenient computationally than searching for minimum lattice energy structures. Related efforts employing Monte Carlo

methods were reported in which the energies of global minima were calculated for one- and two-dimensional aggregates, which can then be compared to the structure of the experimentally observed aggregates in the crystal structure. These studies indicated that the energies for a variety of isolated one-dimensional translation aggregates with structures identical with those observed in crystal structures were less than 2 kcal above the calculated global minima for a particular aggregate. In the case of translation aggregates, the structures of the experimentally observed aggregates were very similar to those corresponding to the calculated global minima.¹⁹ Different conclusions were reached in similar studies of one-dimensional aggregates in which the aggregate molecules were organized by screw, glide, and inversion symmetry operations.²⁰ In these cases the energies of the observed aggregate structures were found to lie as high as 5.7 kcal above the calculated global minima, with visually different structures. This was attributed to packing interactions between the one-dimensional aggregates in the bulk crystal which fill voids in the aggregate but are not accounted for in calculations performed on an isolated aggregate. This concept was extended to two-dimensional translation monolayer aggregates, with the analysis indicating that the gross structural features of the final monolayer structure can be deduced by first calculating the structure of one-dimensional aggregates, with the final conformational details becoming evident upon assembly of the one-dimensional aggregates into the two-dimensional layers.²¹ Although these studies indicate that three-dimensional packing influences the structure of low-dimensional aggregates, they reveal that crystal structures can be dissected into supramolecular low-dimensional assemblies which can be viewed as the building blocks of a crystal lattice.

The formation of nanostructural elements with desired arrangements and dimensionalities relies on an appropriate "topological director," that is, molecules having a well-defined functional group that can recognize complementary functional groups on other like molecules (homomeric assembly) or different molecules (heteromeric assembly). A crucial property of directors is bonding which is strong and highly directional relative to competing interactions. Formation of extended networks, regardless of dimensionality, also requires "polyvalent" modules, that is, molecules having more than one bonding functionality. These capabilities are provided by molecules containing multiple hydrogen-bonding functionalities, which provide "structural algorithms" capable of directing assembly (Figure 1). To a first approximation, these algorithms conform to the geometric requirements and strengths of the hydrogen bonds, which have been examined quite thoroughly by analysis of hydrogen-bonding patterns in molecular crystals.^{22–27}

This principle was reflected in a recent examination of hydrogen-bonded supramolecular aggregates which were classified as having one of four structural motifs: "zero-dimensional" discrete assemblies lacking any translational symmetry, one-dimensional α -networks possessing one degree of translational symmetry, two-dimensional β -networks possessing two degrees of translational symmetry, and γ -networks with three degrees of translational symmetry (Figure 2).²⁸ It was

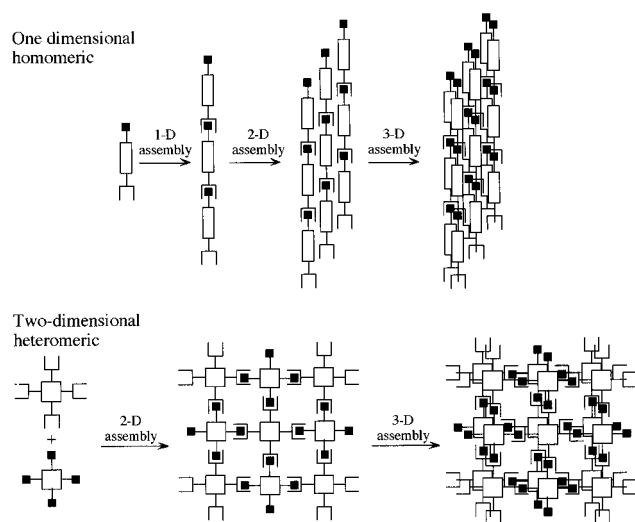


Figure 1. Schematic representations of (a, top) a homomeric hydrogen-bonding assembly formed from molecules with divalent hydrogen-bonding functionality directed along a single dimension and (b, bottom) a heteromeric hydrogen-bonding assembly formed from molecules with tetravalent hydrogen bonding functionality directed in a two-dimensional plane. The topology of an aggregate is defined by the molecular shape and arrangement of functional groups, which defines the dimensionality and symmetry of the motif. Further assembly of these low-dimensional aggregates into three-dimensional crystal lattices occurs by nonspecific intermolecular interactions.

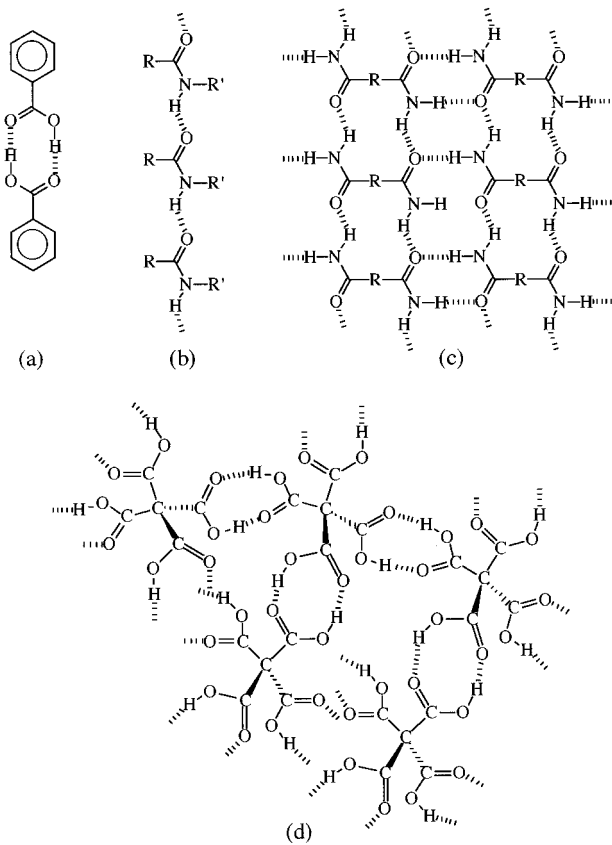


Figure 2. Schematic representation of (a) a discrete assembly of a benzoic acid dimer, (b) a one-dimensional α -network of a secondary amide, (c) a two-dimensional β -network of a primary diamide, and (d) a three-dimensional γ -network formed from methane tetracarboxylic acid.

suggested that low-dimensional networks of proper rod group symmetry could be assembled into higher dimensional ones; for example, the 2-fold symmetry of P2

α -networks favors their assembly into β -networks provided hydrogen-bonding functional groups normal to the one-dimensional 2-fold axis are present.

One-Dimensional Hydrogen-Bonded Aggregates

The simplest hydrogen-bonded nanostructural elements are one-dimensional supramolecular assemblies that can be described as “wires”, “chains”, “tapes”, or “ribbons”. One-dimensional heteromeric hydrogen-bonded helices have also been observed in cocrystals of an aminopyridine and pimelic acid,²⁹ and cocrystals of enantiomerically pure *trans*-1,2-diaminocyclohexanes and enantiomerically pure 1,2-cyclohexanediol.³⁰ A particularly interesting structure containing one-dimensional “tubules”, crystallized by hydrogen bonding between stacked peptide “cylinders”, was also reported recently.³¹

The relationship between the structures of one-dimensional aggregates and their corresponding three-dimensional crystals also can be illustrated by nitroanilines, which typically organize in the solid state as one-dimensional hydrogen-bonded aggregates due to intermolecular contacts between amino protons and nitro proton acceptor sites.³² Head-to-tail hydrogen bonding in nitroaniline chains imparts acentric character to these one-dimensional assemblies, as nitroaniline hydrogen bonds prevent the formation of centers of symmetry. This is particularly favored when the nitro and amino groups are meta or para to each other as ortho substitution can result in the formation of cyclic dimers. If these chains are the primary species present during the initial stages of crystallization owing to hydrogen-bonding interactions, they may serve to bias crystallization toward noncentrosymmetric phases. However, this bias can be compromised by the tendency of the chains to pack centrosymmetrically during their assembly into the three-dimensional crystal lattice. Nevertheless, a survey of the Cambridge Structural Database in 1992 revealed that benzoic acids which organize into acentric chains tend to crystallize into noncentrosymmetric space groups.³³ Benzoic acids aggregate into acentric chains when hydrogen bonds form between a benzoic acid and two or more neighboring benzoic acid molecules, whereas dimers commonly form centric patterns.³⁴ Of 139 structures examined, 118 crystallized as dimers and 21 crystallized with benzoic acid chains. While 98% of the dimers crystallized into centrosymmetric space groups, 52% of the crystals containing acentric chains crystallized into noncentrosymmetric space groups, much greater than the overall occurrence of noncentrosymmetric structures from organic molecules that typically are not centric (ca. 10%). This appears to illustrate that the symmetry of the one-dimensional aggregate introduces a bias toward the crystal packing of the bulk crystal. This principle was exploited in the synthesis of cocrystals of 4-nitrobenzoic acid and 4-aminobenzoic acid, and 4-aminobenzoic acid and 3,5-dinitrobenzoic acid, which organized into acentric chains by carboxylic acid dimerization and weaker hydrogen bonding between the nitro and amino groups (Figure 3).³⁵

One-dimensional heteromeric wires have also been observed recently in salts prepared from a bis(cyclic ammidine) dication (**1**, Chart 1) and terephthalate (**2**) and isophthalate (**3**) dianions (Figure 4).³⁶ The integrity

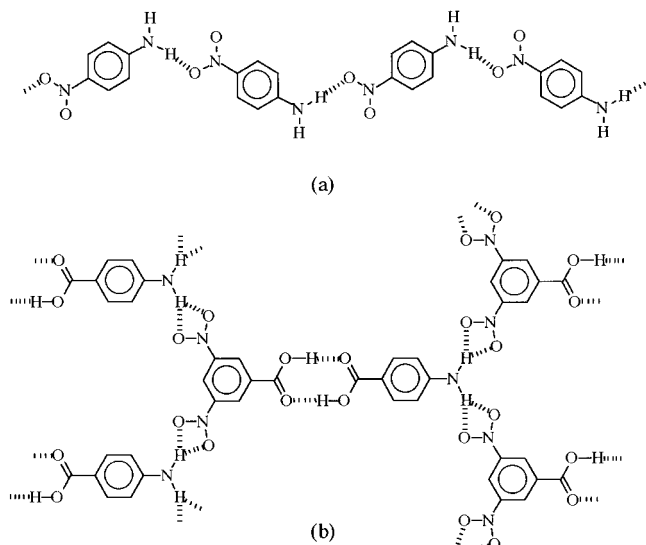
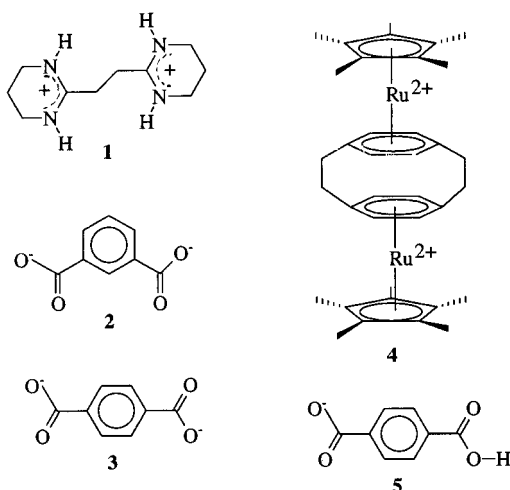


Figure 3. (a) Schematic representation of a heteromeric acentric one-dimensional chain formed from *p*-nitrobenzoic acid and *p*-aminobenzoic acid. (b) Schematic representation of the chainlike aggregate observed in the 1:1 cocrystals of 4-aminobenzoic acid and 3,5-dinitrobenzoic acid. The chain is acentric with the polar direction pointing horizontally.

Chart 1



of this hydrogen-bonded wire is probably reinforced by the ionic charge of the molecular components. These wires were discrete in nature, with no identifiable specific interactions between chains in the bulk crystal. A homomeric hydrogen-bonded chain aggregate was observed in the 1:2 salt of the $[(C_5Me_5)Ru(p\text{-cyclophane})Ru(C_5Me_5)]^{2+}$ (**4**) and the terephthalate monoanion (**5**).³⁷ The single-crystal X-ray structure of this salt reveals one-dimensional chains of terephthalate monoanions hydrogen bonded end-to-end in an infinite chain. The hydrogen-bonded terephthalate chains in this structure belong to the class generally described as Speakman salts,³⁸ which are known to have exceptionally strong hydrogen bonds owing to the enhanced electrostatic attraction between the proton and the carboxylate anion. The hydrogen-bonded chains are oriented parallel to one-dimensional chains of the rodlike dications, which stack by van der Waals interactions. This crystal structure reveals the mutual reinforcement of hydrogen bonding and electrostatic interactions.

Elegant synthetic approaches to robust one-dimensional ribbons and tapes, which may mimic motifs in

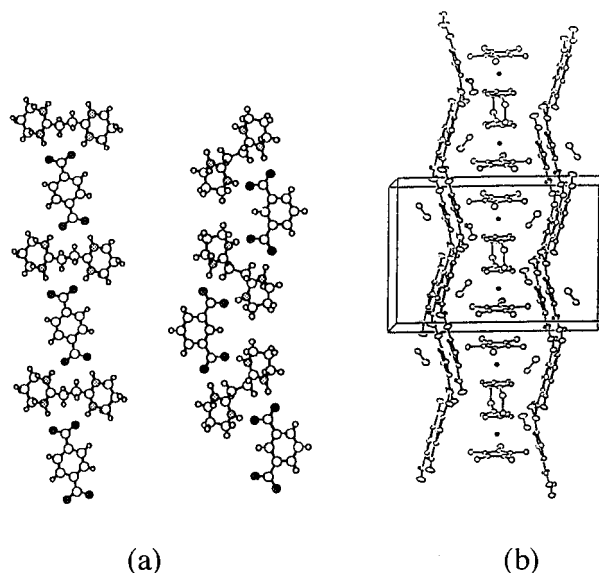


Figure 4. (a) One-dimensional hydrogen-bonded "wires" formed from dication of 1,2-bis(2'-tetrahydropyrimidyl)ethane and terephthalate and isophthalate dianions. Hydrogen bonding between the bisammidinium protons and the carboxylate oxygens of the anions directs the assembly into wires. (b) One-dimensional wires formed by assembly of terephthalate monoanions which enforce the assembly of $[(C_6Me_6)Ru(p\text{-cyclophane})Ru(C_6Me_6)]^{2+}$ cations into one-dimensional stacks.

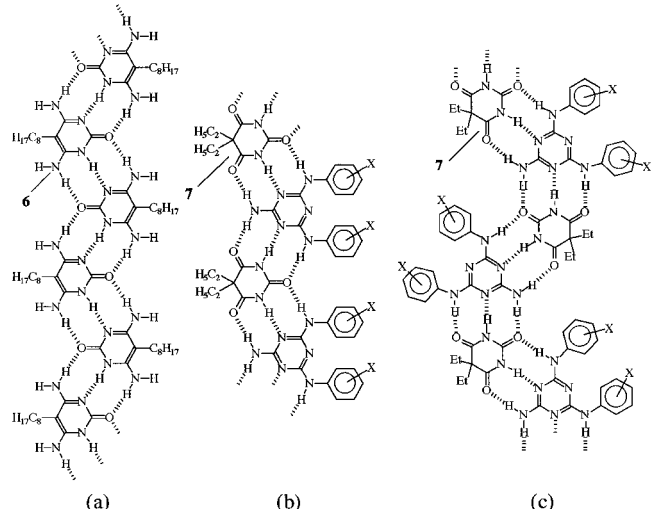


Figure 5. (a) Homomeric hydrogen-bonded linear ribbon of **6**, (b) a heteromeric linear "tape" motif observed for 5,5-diethylbarbituric acid and substituted tris(amino)pyrimidines with $X = p\text{-}(H, F, Cl, Br, I, CH_3, CF_3)$ and $m\text{-}(H, F, I, CH_3, CF_3)$, and (c) a heteromeric "crinkled tape" motif observed for 5,5-diethylbarbituric acid and substituted triaminopyrimidines with $X = p\text{-}CO_2Me$ and $m\text{-}(Cl, Br)$.

related two-dimensional materials, have been reported recently in which the dimensionality is constrained by introduction of blocking functional groups on the molecular components. These blocking groups serve to prevent further assembly of the one-dimensional aggregates into two-dimensional networks, some of which are described in the following section. For example, homomeric linear chains were observed for 4,6-diamino-5-octylpyrimidin-2(1*H*)-one (**6**) and 5,5-diethylbarbituric acid (**7**) in which the octyl and ethyl groups block assembly into two-dimensional sheets (Figure 5).^{39,40} Heteromeric linear tapes were observed for the 1:1 cocrystal of **7** and 5-butylpyrimidine-2,4,6-triamine (**8**).

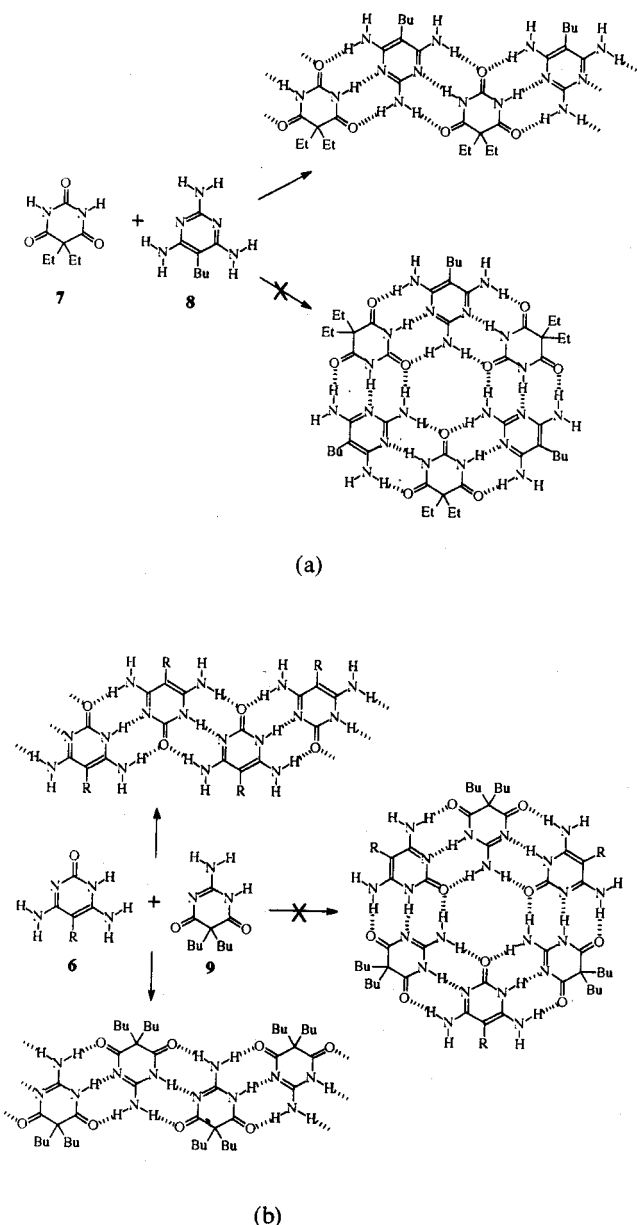


Figure 6. (a) Assembly of 5,5-diethylbarbituric acid and 5-butylpyrimidine-2,4,6-triamine results in heteromeric ribbons in the crystalline solid state, but the cyclic hexamer rosette is not observed even though the number of hydrogen bonds is identical with that in the ribbon. (b) Mixtures of 4,6-diamino-5-octylpyrimidin-2(1H)-one and 5,5-dibutylpyrimidine-4,6(1H)-dione afford only crystals of the homomeric ribbons, not 1:1 cocrystals containing heteromeric ribbons or cyclic hexamers.

An alternative possibility, the cyclic hexamer “rosette”, was not observed. Attempts to make a 1:1 cocrystal of **6** and 5,5-dibutylpyrimidine-4,6(1H)-dione (**9**), which can form only a rosette, were unsuccessful as only the homomeric chains were observed to crystallize from mixtures of the two compounds. The linear tape and rosette networks are identical in terms of fulfilling hydrogen-bonding sites, strongly suggesting that solid-state packing of the rosette aggregate is not as efficient as that of the tapes. However, a rosette pattern was observed for a differently substituted heteromeric system.⁴¹ The effect of packing on one-dimensional modules is also evident from the structures of a series of heteromeric aggregates based on **7** and substituted triaminopyrimidines (Figure 6).^{42,43} These aggregates

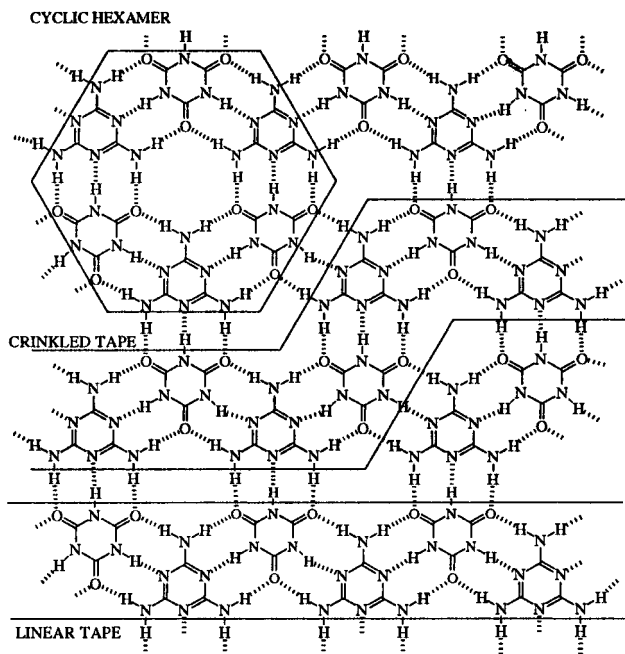
exhibited either linear or “crinkled” tape motifs depending upon the size of the pyrimidine substituents and the position (i.e., meta or para substituted), clearly a consequence of the efficiency of three-dimensional packing of the tapes. Related behavior was observed in an exhaustive examination of cocrystals of urea and linear α,ω -dinitriles with the formula $\text{NC}(\text{CH}_2)_n\text{CN}$. These cocrystals form 1:1 layered motifs for $n = 3-5$ but commensurate or incommensurate channel inclusion compounds for $n = 6, 8, 10$, and 12.⁴⁴ The observation of different motifs was attributed to the competition between hydrogen bonding and packing efficiency, with the greater packing efficiency of the channel compounds outweighing the favorable hydrogen bonding in the layered motifs for large n . These observations indicate that when more than one hydrogen-bonding motif is possible for a given low-dimensional assembly, crystal packing energies can influence the choice the system makes. Nevertheless, the persistence of a limited number of hydrogen-bonding motifs suggests that these networks can reduce the available packing options during crystallization, thereby simplifying crystal design.

Two-Dimensional Hydrogen-Bonded Networks

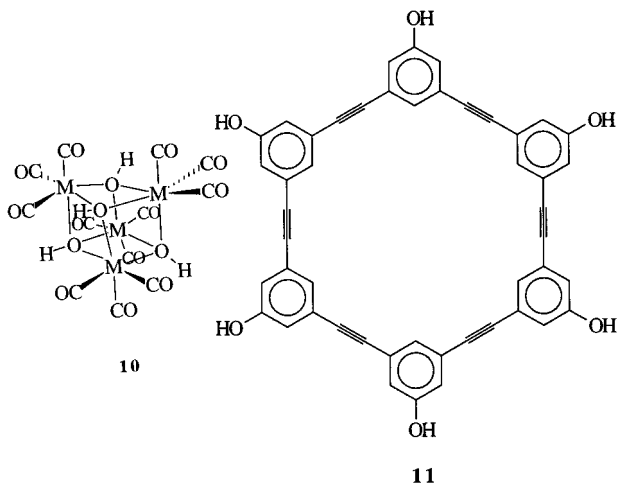
Two-dimensional networks based on hydrogen bonding require polyvalent planar molecules having three or more hydrogen-bonding functionalities. These networks can be either homomeric or heteromeric and, if robust, can be considered to be the crucial nanostructural elements involved in the formation of a three-dimensional crystal. Assembly of flat two-dimensional sheets into a crystal lattice generally will occur by layering in a manner that allows molecular protrusions from one sheet to nestle in hollows in sheets above and below in order to maximize van der Waals interactions. It has been suggested that the structure of a sheet composed of molecules held together only by weak nondirectional dispersive interactions will be that corresponding to best packing in the third dimension.²⁰ However, it is likely that the structure of hydrogen-bonded sheets would be less affected by interactions with adjoining sheets, although the layering of equivalent sheets generally will allow protrusion-hollow packing by simple translation symmetries.

The prototypical example of a two-dimensional network is pure trimesic acid (benzene-1,3,5-tricarboxylic acid),⁴⁵ which crystallizes to form two-dimensional infinite “honeycomb” grids due to hydrogen bonding between the carboxylic acid groups. This arrangement leads to large two-dimensional voids formed by rings of six trimesic acid molecules. However, these voids are filled by interpenetration of three parallel rings from other symmetry equivalent networks, illustrating how the design of a strictly two-dimensional material can be frustrated by the tendency to maximize the packing fraction. Recently, the formation of noninterpenetrated trimesic acid networks was achieved by crystallizing trimesic acid in the presence of pyrene.⁴⁶ Layered networks of trimesic acid assembled around pyrene guest molecules, resulting in the formation of one-dimensional channels filled with stacks of pyrene molecules. An illustrative example of a heteromeric two-dimensional network is the one proposed for the 1:1 cocrystal of melamine and cyanuric acid (CA-M).⁴⁷ The

polymeric nature of this material has prevented isolation of single crystals of quality sufficient for X-ray diffraction. However, the motifs present in this hypothetical network have been duplicated in the aforementioned rosettes, linear tapes, and crinkled tapes.



Two-dimensional networks were observed in cocrystals of $[\{M(CO)_3(\mu_3-OH)\}_4]$ (**10**, M = Mn, Re) and "spacer" molecules diaminopropane, hexamethylenetetramine, or 4,4'-dipyridine (Figure 7).⁴⁸ These spacer



molecules served as hydrogen-bonding acceptor sites for the hydroxyl groups extending from the corners of the pseudotetrahedral organometallic cubanelike molecules. The polyvalency of the two components enabled formation of polymeric open "chicken-wire" networks with a substantial amount of void space. In the case of the 4,4'-dipyridine spacer, these voids were filled with solvent molecules. Two-dimensional networks also have been observed in cocrystals of the alicyclic diols and *p*-chlorophenol, in which the two molecules are organized into layers by hydrogen bonding between hydroxyl groups.⁴⁹ The macrocycle **11** formed crystalline two-dimensional networks by hydrogen bonding between the phenol groups, with further hydrogen bonding to either

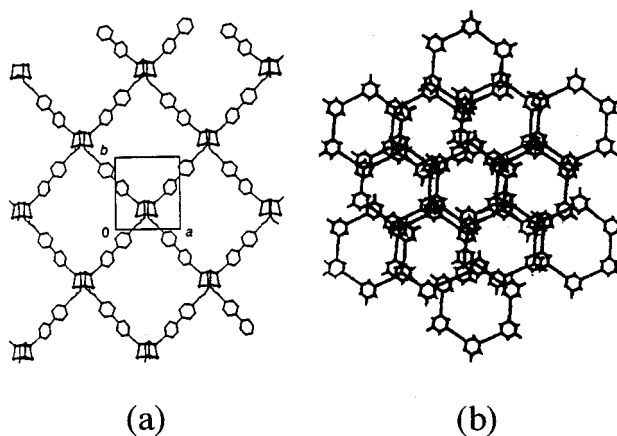


Figure 7. (a) Two-dimensional "chicken-wire" motifs observed in $[\{Re(CO)_3(\mu_3-OH)\}_4] \cdot 2\text{-}(4,4'\text{-dipyridine}) \cdot MeOH$. (b) Three layers of two-dimensional networks of the macrocycle **11** which stack in an ...ABCABC... cubic closest-packing motif.

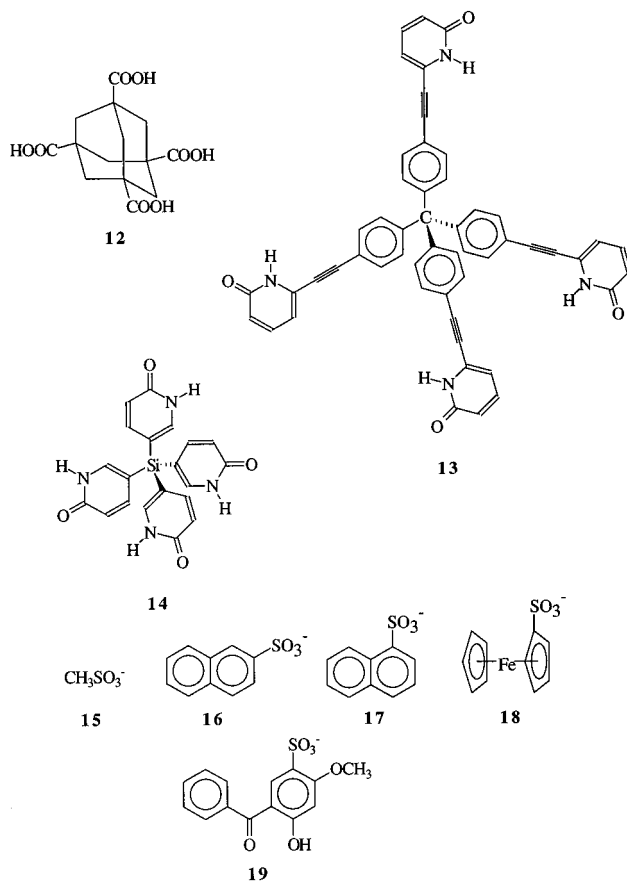
methanol or ethanol solvent molecules suggested by the data.⁵⁰ These layers stacked in an ...ABCABC... motif so as to form one-dimensional 9 Å diameter channels.

Three-Dimensional Hydrogen-Bonded Networks

Molecular crystals with three-dimensional networks are intriguing for a variety of fundamental and practical issues. Such networks are aesthetically pleasing and can provide insight into the principles governing the assembly of molecular networks. Three-dimensional molecular networks with nanometer scale voids would mimic structurally inorganic zeolites. Consequently, such materials may accommodate guest molecules with desirable optical properties, separate small molecules based on size exclusion or chemical affinity, or provide tailored reaction environments for included molecules. Zeolite networks are stable toward collapse because of the strength of covalent metal–oxygen bonds and the isotropic nature of the networks. However, the formation of molecular crystals with open network structures typically is frustrated by nature's tendency to avoid empty space and relatively weak, nondirectional interactions. Consequently, nanoscale voids in molecular crystals commonly collapse if emptied of reinforcing guest molecules. Nevertheless, this has not dissuaded crystal engineers from pursuing low-density molecular networks. Strategies for the synthesis of nanoporous crystals have included frustrating molecular packing in the solid state by using molecules with clumsy shapes that cannot be conveniently packed⁵¹ and trapping organic guest molecules in cylindrical, continuous channels formed by host lattices such as urea and tri-*o*-thymotide.^{52–54}

More recently, several research groups recently have prepared hydrogen-bonded three-dimensional nanoporous molecular crystals from tetrahedral or pseudotetrahedral polytopic modules. This work is motivated, at least partially, by three-dimensional diamondoid lattices observed in topologically similar elemental and inorganic crystalline solids such as carbon, ice, and KH_2PO_4 (KDP), which are mechanically strong and have relatively high melting points. The construction of analogous hydrogen-bonded networks requires molecules or aggregates with hydrogen-bonding groups capable of directing assembly in three dimensions. Void

Chart 2



sizes will be governed by the size of the principal building block, in this case by the distance between hydrogen-bonding groups on each building block or the size of spacer molecules inserted between these molecules.

Some of the earliest examples of a molecular hydrogen-bonded diamondoid network are those formed from methanetetraacetic acid⁵⁵ and adamantane-1,3,5,7-tetracarboxylic acid (**12**, Chart 2),⁵⁶ which have pseudotetrahedral topologies (with respect to the arrangement of hydrogen-bonding acid groups). In the case of adamantane-1,3,5,7-tetracarboxylic acid, the network contains voids that are so large that each void is penetrated by four other symmetry-equivalent diamondoid networks, similar to the aforementioned trimesic acid structure (Figure 8). Modulation of the structure of the tetracarboxylic acid revealed that the degree of interpenetration, and subsequent clathration of guest molecules, could be controlled rationally.⁵⁷ The single-crystal X-ray structures of inclusion complexes of 2,6-dimethylideneadamantane-1,3,5,7-tetracarboxylic acid and various organic guest molecules revealed that the steric bulk of the methylidene groups was sufficient to inhibit interpenetration so that only double-diamond structures formed, with the liberated void space filled by the guest molecules. Topologically similar adamantoid networks also have been observed for 1:1 complexes of diamines and quinones.⁵⁸

This principle has been extended recently to other hydrogen-bonding diamondoid directors, referred to as "molecular tectons", with pseudotetrahedral topologies with respect to the hydrogen bonding groups. For example, the 2-pyridone group of **13** formed hydrogen-

bonded dimers with other like molecules, assembling into an infinite diamondoid network with channellike voids.⁵⁹ These voids clathrated either butyric acid, isobutyric acid, valeric acid, or isovaleric acid, depending upon which acid was present in the crystallization solvent. This work has been extended recently to analogues such as **14**, which also formed diamondoid networks with a variety of clathrated organic acids (Figure 8).⁶⁰ The degree of interpenetration differed for **13** and **14**, with **13** being 7-fold interpenetrating and **14** being doubly interpenetrating, leading to an exceptionally large void volume. Removal of the clathrated guest molecules resulted in collapse of the structure owing to the inability of the lattice to withstand the large void volume, but the network was porous enough to allow exchange of guest molecules (i.e., valeric acid with acetic acid). Diamondoid networks have been reported in cocrystals of **10** ($M = Mn$) \cdot 2(bipyridine) \cdot 2CH₃CN and **10** ($M = Re$) \cdot 2(1,4-diaminobenzene) \cdot 4CH₃CN, assembled by hydrogen bonding between the hydroxyl protons of the pseudotetrahedral director and the nitrogen acceptor sites of bipyridine and 1,4-diaminobenzene. The different sizes of the spacer molecules results in different amounts of clathrated CH₃CN molecules.⁶¹ An analogous structure assembled from **10** and the spacer 1,2-diaminoethane has been reported in which enclathration was prohibited by interpenetration of three symmetry-equivalent diamondoid networks.⁶² Interestingly, the same organometallic cubanelike molecules formed two-dimensional networks with other spacer molecules (vide supra), demonstrating the sensitivity of the dimensionality to spacer molecule geometry. A recent review⁶³ describes the relationship between these hydrogen-bonded diamondoid networks and topologically similar molecular networks assembled by covalent interactions.^{64–66} These studies have illustrated that three-dimensional networks based on molecular topological directors may lead to materials capable of selective clathration with structural and mechanical robustness, controllable void volumes, and adjustable microporosity.

Building Three-Dimensional Networks from Two-Dimensional Modules

While the synthesis of three-dimensional networks based on the aforementioned polytopic molecules has been reasonably successful, precise control of crystal packing, network interpenetration, and enclathration of guest molecules can be elusive owing to molecular flexibility and the contribution of weak, nondirectional dispersive interactions which can influence the assembly of independent networks in the crystal. An alternative approach to the synthesis of three-dimensional networks is to use robust two-dimensional hydrogen-bonding networks that serve as nanostructured modules which maintain their integrity during assembly along the third dimension, thereby reducing crystal engineering to one dimension and limiting the number of variables in assembly. However, the assembly of flat molecular sheets typically is governed simply by close packing between protrusions and hollows, and functionality is limited to that contained within the sheets. Functional groups which project from the two-dimensional sheets could direct layer assembly by specific interactions which need not conform to close

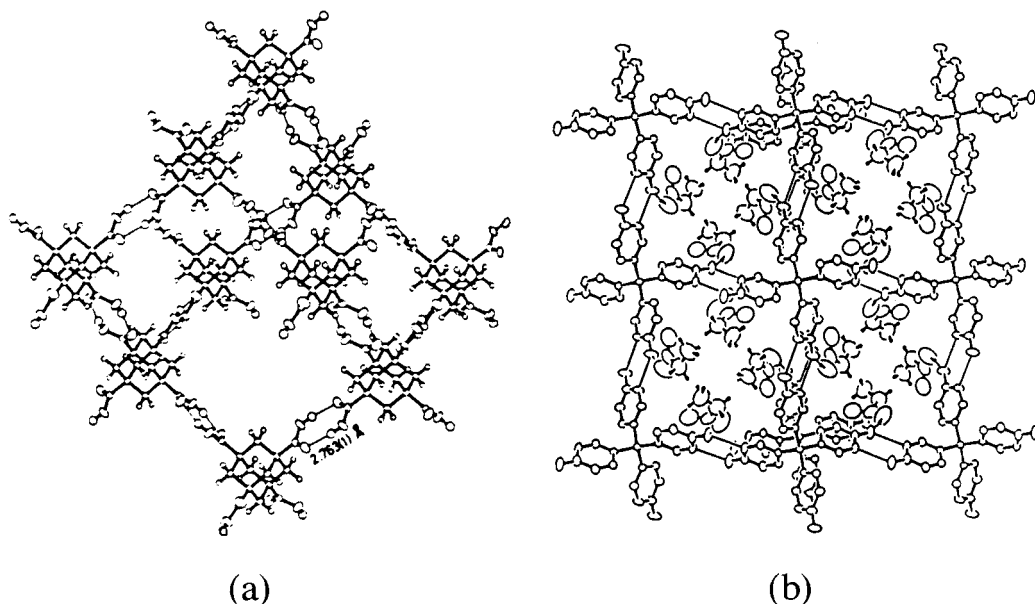


Figure 8. (a) Three-dimensional single diamondoid network in adamantane-1,3,5,7-tetracarboxylic acid. Each void is interpenetrated by four other independent, but symmetry-equivalent, diamondoid sublattices. (b) Segment of the diamondoid network observed in single crystals of **14**·4CH₃CH₂COOH as viewed parallel to the channels.

packing, while introducing function to the material. These interactions may include hydrogen bonding, metal–ligand bonding, covalent bonding, or van der Waals interactions.

We reported recently a relatively simple system based on guanidinium cations and alkane- and arenesulfonate anions which contains these features.^{67,68} The topological equivalence of these ions and strong (guanidinium)N–H \cdots O(sulfonate) hydrogen bonds resulted in the formation of quasihexagonal two-dimensional networks, with the organic residue of the sulfonate anion extending from the guanidinium-sulfonate sheet (Figure 9). The robustness of this network was evident from its presence in over 30 crystalline salts synthesized from a rather diverse variety of sulfonates (Table 1). The integrity of the hydrogen-bonding network was attributed to the identical topologies of the two ions, their similar sizes which allowed for optimum hydrogen-bonding geometries, the maximization of hydrogen bonds because of six guanidinium protons and six electron lone pairs on the three sulfonate oxygen atoms, and electrostatic interaction between the oppositely charged ions. These two-dimensional sheets can be viewed as assembling from one-dimensional ribbons in which the ribbons are connected by a hydrogen-bonding “hinge” parallel to the ribbon axes. In many salts the guanidinium–sulfonate network was perfectly planar ($\theta_{IR} = 180^\circ$). However, many of these salts had sheets which were “puckered” about the hydrogen-bonding hinge, resulting in “accordion” or “pleated” sheets ($\theta_{IR} < 180^\circ$).

The layering motifs observed for the guanidinium–sulfonate salts can be illustrated by the salts containing methanesulfonate (**15**), 2-naphthalenesulfonate (**16**), 1-naphthalenesulfonate (**17**), and ferrocenesulfonate (**18**). Guanidinium methanesulfonate crystallized as large sheets having centimeter dimensions. Single-crystal X-ray structural analysis reveals the presence of two-dimensional quasihexagonal sheets parallel to the *ab* plane which assemble as bilayers (Figure 10). Consequently, the stacking sequence of the sheets

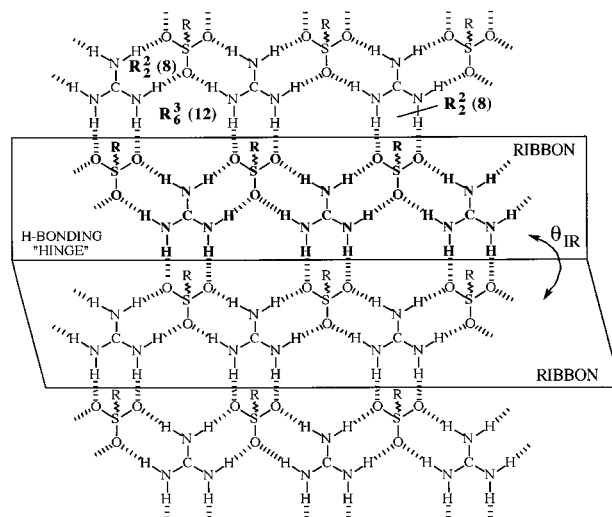


Figure 9. Schematic representation of the quasihexagonal hydrogen-bonding network formed from guanidinium cations and alkyl- or arylsulfonate anions. Hydrogen bonding between the six protons of each guanidinium cation and the six lone-pair electron acceptors of each sulfonate residue, and the 3-fold symmetry of both cations results in an extended network with 3-fold symmetry. The motif can be described as infinite hydrogen-bonded ribbons, depicted in bold, which form from R₂2(8) guanidinium–sulfonate dimers, with adjacent ribbons joined by hydrogen bonding through R₂2(8) dimers and R₆3-(12) rings. The ribbons thereby are connected by a hydrogen-bonding “hinge” which allows puckering of the sheet about an axis parallel to the ribbon in some structures. The puckering is defined by the interribbon (IR) dihedral angle between adjacent ribbons, θ_{IR} . The orientation of the R groups extending from the sulfonate residues is not specified.

comprises a nonpolar region in which the methyl groups hold the sheets together by van der Waals interactions and a polar region between the sheets in which Coulombic and van der Waals interactions are operative. The salt formed from 2-naphthylsulfonate crystallizes in the same motif, but with a slight puckering of the two-dimensional sheets ($\theta_{IR} = 146^\circ$ vs 180°) and a larger bilayer “thickness” compared to the methanesulfonate compound (10.82 vs 5.96). Both differences were at-

Table 1. Layering Motifs for Selected Guanidinium Alkane- and Arenesulfonates

<chem>CH3SO3^-</chem>	bilayer	180
<chem>CF3SO3^-</chem>	bilayer	180
<chem>CH3CH2SO3^-</chem>	bilayer	180
<chem>CH3(CH2)3SO3^-</chem>	single layer	157
	single layer	122
<chem>c1ccccc1[SO3^-]</chem>	bilayer	150
<chem>c1ccc2ccccc2[SO3^-]</chem>	single layer	77
<chem>c1ccc2ccccc2[SO3^-]</chem>	bilayer	146
	single layer	153
<chem>Cc1ccc(cc1)[SO3^-]</chem>	bilayer	151
<chem>Nc1ccc(cc1)[SO3^-]</chem>	bilayer	147
<chem>OCc1ccc(cc1)[SO3^-]</chem>	bilayer	164
<chem>O=[N+]([O-])c1ccc(cc1)[SO3^-]</chem>	single layer	72
<chem>OCc1ccc(cc1)[SO3^-]</chem>	single layer	51
<chem>OC(=O)c1ccc(cc1)[SO3^-]</chem>	nonlayered	
<chem>Cc1ccc(cc1)[SO3^-]</chem>	single layer	88
	single layer	86
<chem>c1ccc(cc1)[SO3^-]N</chem>	bilayer	150
<chem>c1ccc(cc1)[SO3^-]N</chem>	bilayer	150
<chem>O=[N+]([O-])c1ccc(cc1)[SO3^-]</chem>	nonlayered	
<chem>O=[N+]([O-])c1ccc(cc1)[SO3^-]N</chem>	nonlayered	
<chem>O=[N+]([O-])c1ccc(cc1)[SO3^-]N</chem>	single layer	165

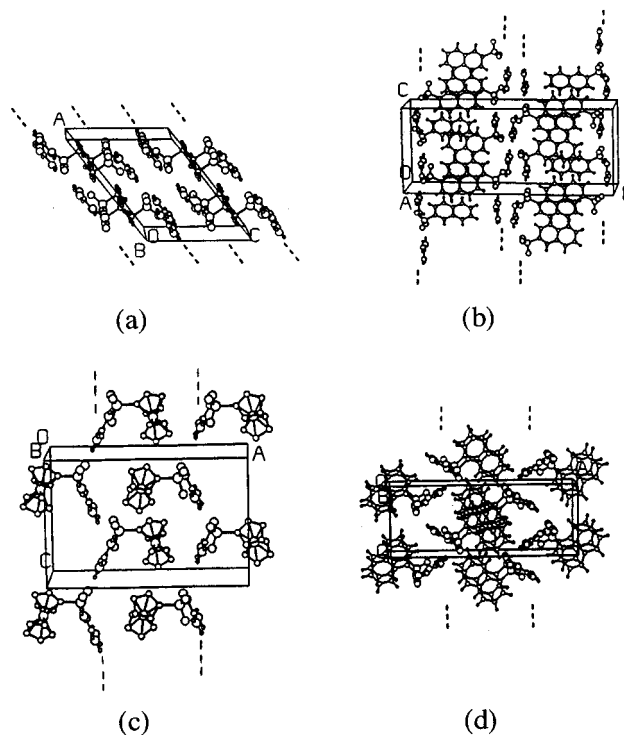


Figure 10. Unit cells of (a) guanidinium methanesulfonate, (b) guanidinium 2-naphthylsulfonate, (c) guanidinium ferrocenesulfonate, and (d) guanidinium 1-naphthylsulfonate, as viewed along the hydrogen-bonded sheets. (a) and (b) assemble as bilayers, whereas (c) and (d) assemble as translationally related single layers. Both motifs exhibit interdigititation of the R groups which provides a "van der Waals" glue which holds the hydrogen-bonded sheets together. The dashed lines represent the mean plane of the hydrogen-bonded sheet.

tributed to the greater steric demands of the naphthalene residue compared to the methyl group. The puckering results from bending of adjacent ribbons as if the hydrogen bonds between the ribbons act as a hinge. The bilayer structure is evident from the macroscopic properties of these crystals, as crystals can be cleaved with a razor along the sheet direction, or simply by pulling the sheets apart with adhesive tape applied to opposite sides of a crystal. Atomic force microscopy of freshly cleaved crystals of guanidinium methanesulfonate in a saturated solutions of the salt also revealed large molecularly flat *ab* faces with molecular-scale contrast having hexagonal symmetry (Figure 11).

The assembly of guanidinium salts of ferrocenesulfonate and 1-naphthalenesulfonate differed dramatically from the aforementioned salts with respect to two principal features. These salts did not form bilayers; rather, the hydrogen-bonded sheets stacked by interdigititation of translationally related single layers, in which the R groups on adjacent ribbons within a sheet orient to opposite sides of the sheet (Figure 10). The appearance of two different motifs was attributed to the different steric requirements of the R groups extending from the hydrogen-bonded sheets. The interdigitated bilayer motif of the methanesulfonate and 2-naphthylsulfonate salts is observed because interdigititation of the R groups within the bilayer is possible even with all the R groups are oriented on the same side of the hydrogen-bonded sheet. If the R groups are described by cylinders it can be shown that interdigititation of the R groups of opposing sheets is possible if the diameter of R, as viewed normal to the hydrogen bonded

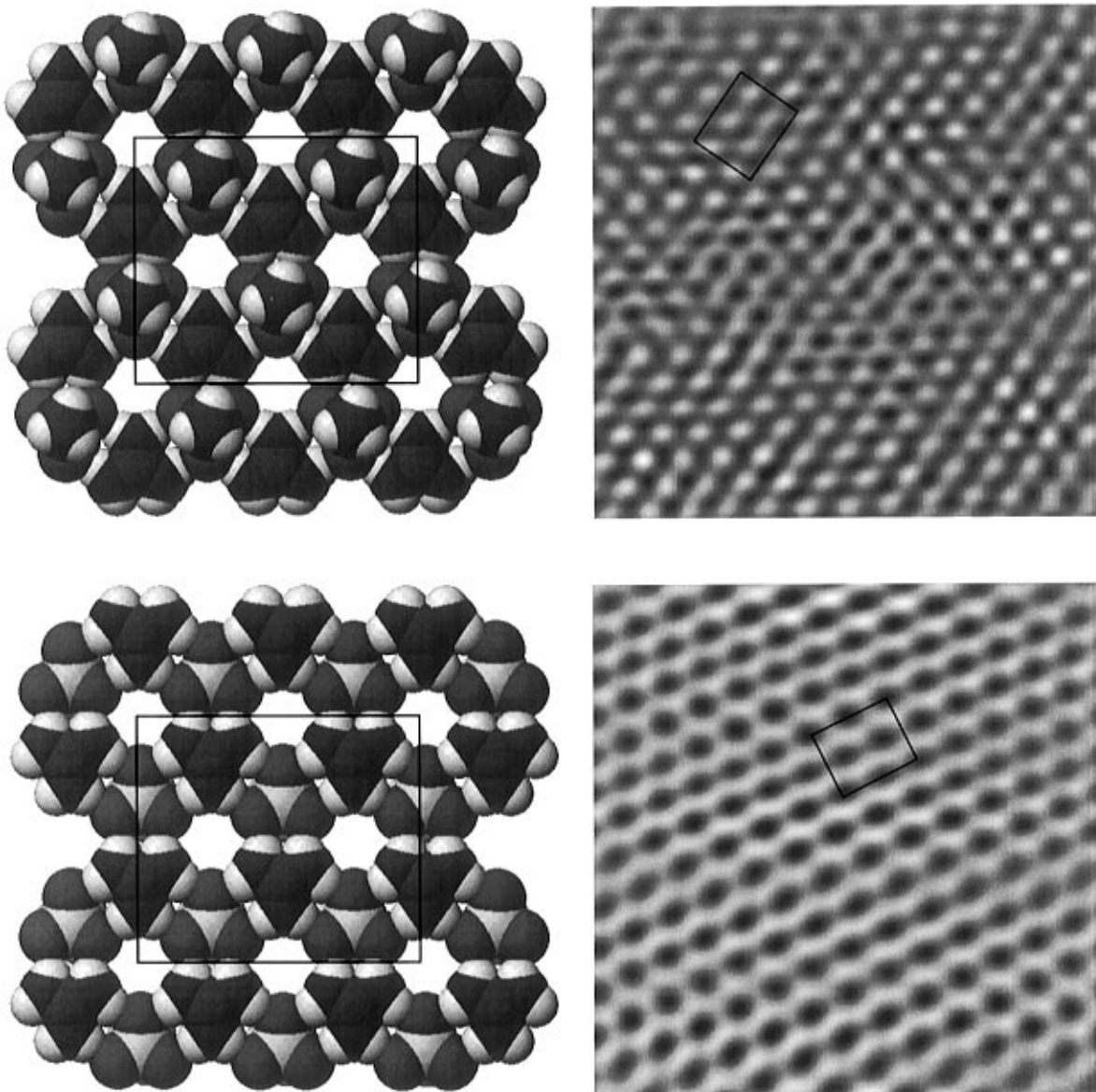


Figure 11. Space filling views of the surface of the hydrogen-bonded guanidinium methanesulfonate sheet as viewed looking down at side containing the methyl groups (top left) and the opposite side where only the hydrogen-bonded network is observed (bottom left). To the right of each figure is an atomic force microscope image which appears to correspond to the molecular contour of each surface, although such assignments can be risky because AFM data represent a convolution of the tip shape and sample surface contour. Nevertheless, the image assigned to a methyl "up" surface (top right) exhibits isolated nearly circular features with dimensions comparable to a methyl group, whereas the image assigned to the hydrogen-bonded network (bottom right) clearly shows the quasihexagonal network. The rectangular boxes in each panel has dimensions of $14.8 \times 12.8 \text{ \AA}$.

sheet, is less than $d_{S-S}/\sqrt{3}$, where d_{S-S} is the center-to-center distance between nearest sulfonate residues (Figure 12). If the diameter exceeds this value interdigitation is not possible and the salts resort to the single layer motif in order to achieve dense packing. The R groups also interdigitate in this motif, albeit in a different manner than in the bilayer structure. The naphthalenesulfonates are particularly illustrative: 1-naphthylsulfonate has the larger projected area and therefore forms the single layer rather than the bilayer motif. A single layer motif was also observed for the rather large 5-benzoyl-4-hydroxy-2-methoxybenzenesulfonate anion (**19**). Recent AFM investigations in our laboratory revealed ordered adlayers of **19** on the surface of hydrotalcite, a layered clay with two-dimensional cationic metal hydroxide sheets.⁶⁹ The AFM and X-ray diffraction studies suggested that the anion layer motif in the guanidinium salt was similar

to that in the intercalate region between the metal hydroxide sheets of hydrotalcite, particularly with respect to the anion orientation.

Analysis of the hydrogen bonding distances and geometries in the guanidinium organosulfonate salts indicated that even the most puckered sheets could be considered as continuous two-dimensional networks. The puckering reflects flexibility in this motif which can relieve tensile or compressive stresses resulting from steric interactions (for large R) or inefficient packing (for single-layer motifs with small R), respectively, between organic residues in the bilayer region. *We believe that this feature is critical to the persistence of this two-dimensional network for a rather diverse variety of sulfonates.* Without this flexibility to accommodate differently sized R groups, assembly of a two-dimensional guanidinium–sulfonate network would be inhibited and nonlayered phases would form. We have

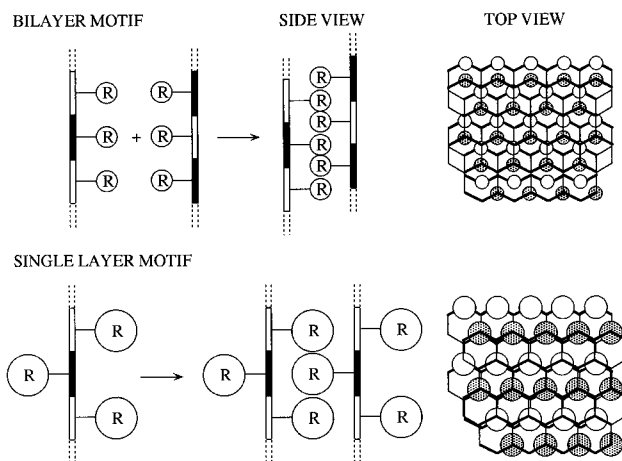


Figure 12. Schematic representation of the steric influence of the R group on the layering motif in guanidinium-sulfonate salts. Interdigititation of R groups all arranged on the same side of the hydrogen-bonded sheet is possible if the R group projected diameter is $< d_{S-S}/\sqrt{3}$, where d_{S-S} is the distance between nearest sulfonate groups. This results in the bilayer structure (top). If the diameter is $> d_{S-S}/\sqrt{3}$, interdigititation is not possible and the single layer motif, in which R groups on adjacent ribbons are oriented to opposite sides, is formed as this allows interdigititation and efficient packing between the hydrogen-bonded sheets. Note that only the R groups in the layer interior are depicted in the normal views on the right.

observed nonlayered structures only in a limited number of examples, but these are a consequence of *direct* steric or hydrogen-bonding interactions between the two-dimensional sheet and sulfonate functional groups, such as ortho or para substituents on benzenesulfonates. The intrinsic robustness of this two-dimensional network simplifies crystal engineering as assembly needs to be understood and controlled only in the third remaining dimension. Consequently, this two-dimensional network can be considered as a nanostructured “supermolecule” for the supramolecular synthesis of a three-dimensional crystal.

The crystal structures of the alkane- and arenesulfonates revealed that the layering motifs in the third dimension were governed by the tendency to achieve efficient packing within the bilayer. In these cases, there was one R group for every sulfonate ion in each layer. However, if disulfonates were used to bridge hydrogen bonded sheets the density of R groups would be reduced by a factor of 2, creating void space in the bilayer region (Figure 13). Indeed, we have determined recently that for $n = 0, 2$, and 4 , covalently linked bilayers with quasihexagonal planar hydrogen-bonding sheets ($\theta_{IR} = 180^\circ$) are formed.⁷⁰ The ethanesulfonate has a considerable amount of void space between the layers, the crystal overall having a packing fraction of 0.59. The butanesulfonate salt has larger void spaces which are manifested in the form of one-dimensional channels occupied by acetonitrile solvent molecules from the crystallization solvent. In this case, the presence of one-dimensional channels is ensured by the topology provided by the one-dimensional ribbons contained in the hydrogen-bonded sheets. The packing fraction of the network without solvent is 0.51, whereas with solvent it is 0.68, which is more typical of organic crystals. Interestingly, the propanedisulfonate salt exhibited a nonlayered solid-state packing. We have concluded from these observations that the hydrogen-bonded network is sufficiently robust so that the the

low packing fraction of 0.59 for $n = 2$ can be tolerated. The void space for $n = 3$ apparently is too large to be sustained but too small to accommodate solvent to stabilize the bilayer motif. However, for $n = 4$ the void space is large enough to accommodate solvent molecules which act to buttress the bilayer. We are now examining whether more extensive pillaring of the hydrogen-bonded sheets can be realized by using longer disulfonates coupled with solvent or guest molecules having lengths comparable to the expected separation between the sheets. These efforts have led to the recent synthesis in our laboratory of similar pillared networks based on biphenyl-4,4'-disulfonate and 1,6-naphthalene disulfonate. Both systems possess large one-dimensional channels, with the biphenyl compound clathrating either aromatic guests or methanol and the naphthalene compound selectively clathrating linear functionalized alkane guests such as alkane nitriles, dinitriles, and alcohols.⁷¹ We anticipate that the guanidinium sulfonates will prove to be versatile hosts because the two-dimensional hydrogen-bonded sheet is robust enough to be treated as a reliable nanostructured module and, consequently, crystal design relies only on changes in one dimension. *Another advantage of this approach to nanoporous crystals is that interpenetration is prohibited for the covalently linked bilayers.* Furthermore, the diverse variety of disulfonates available commercially or by synthesis can be exploited to systematically adjust the void environment and the function of the layers.

Crystalline Nanostructures with Function

The use of reliable, robust nanostructured modules in crystal engineering will likely lead to improvements in the design and synthesis of functional molecular materials. While it is tempting to compare nanoporous molecular crystals with inorganic aluminosilicate zeolites, such a comparison is contentious because presently the molecular networks cannot approach the thermal and structural stability of their inorganic counterparts. However, the materials are similar with respect to their clathration properties, with differences only in the method of preparation; zeolitic guest–host materials are prepared by adsorption of guests into preformed stable voids, whereas clathration by the molecular networks must occur during crystallization of the host lattice. Crystallization routes may be advantageous in some cases as the clathration usually will occur in near perfect yield without diffusion limitations that can be problematic in zeolites. The molecular nature of these voids provides unique opportunities with respect to systematically adjusting the void environment by molecular design, which can be exploited to tune electronic properties and arrangement of the guest molecules. The energy of transition states for reactive processes can be modified by varying the network environment, for example, by controlling the polarity of the voids through judicious selection of organic functionality. Finally, if reactions are performed in these networks, the reaction products can be retrieved by simply dissolving the host network under mild conditions, compared to the rather harsh conditions required to dissolve inorganic zeolites.

Modular design based on robust nanostructures may facilitate the organization of molecular into motifs required for desired functions such as light harvesting

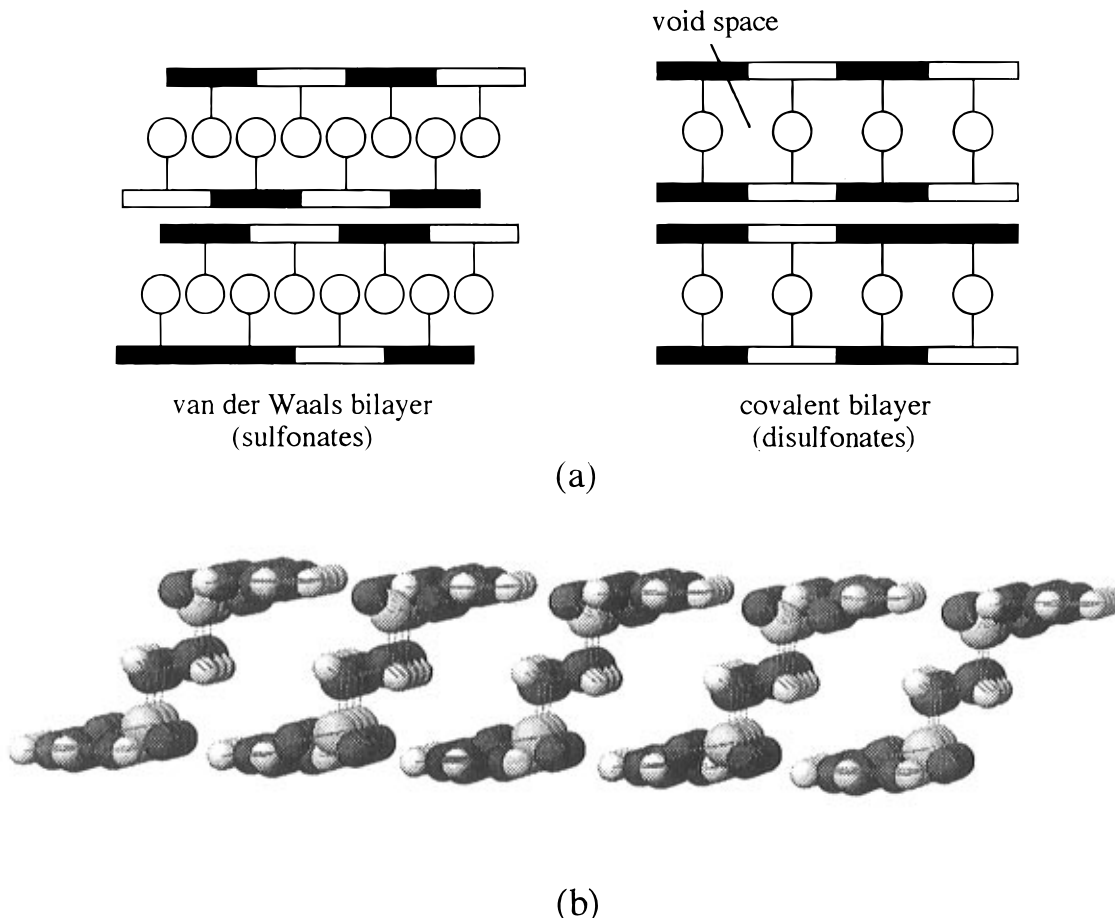


Figure 13. (a) Schematic representation of void volume created in a guanidinium sulfonate bilayer by replacing alkanesulfonates with alkanedisulfonates. (b) Layered motif of the nanoporous guanidinium ethanesulfonate salt.

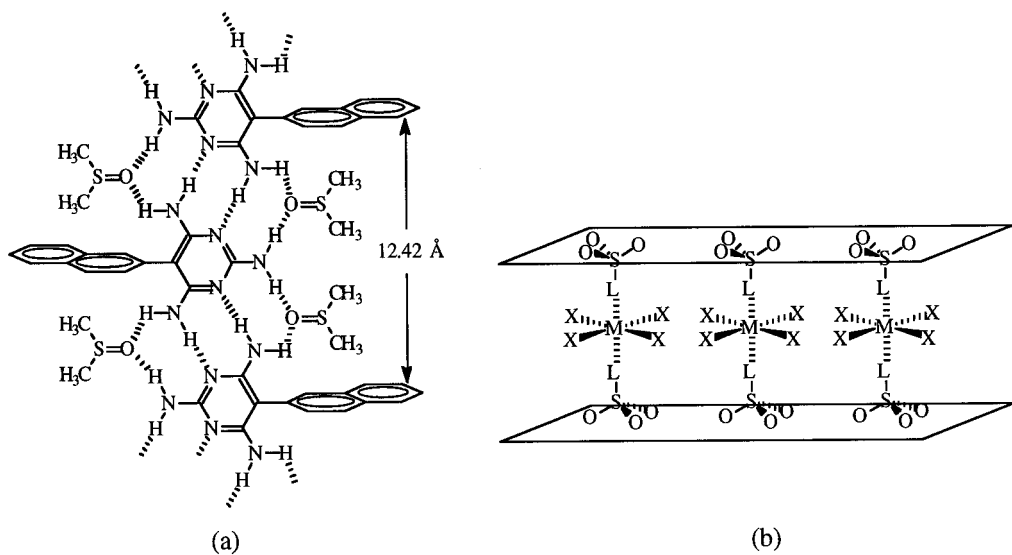


Figure 14. (a) Solvated homomeric ribbon of 5-(1-naphthylmethyl)pyrimidine-2,4,6-triamine. (b) Schematic representation of a two-dimensional guanidinium-sulfonate network in which the sulfonate residue ligates a generic metal complex so that the metal complex is integrated into the bilayer region as an ordered array.

and energy transfer, nonlinear optical behavior, magnetism, or conductivity. The robust hydrogen-bonded homomeric ribbon motif observed for substituted pyrimidine-2,4,6-triamines has been duplicated in crystals of 5-(1-naphthylmethyl)pyrimidine-2,4,6-triamine (Figure 14).³⁹ The ribbons incorporate dimethyl sulfoxide by hydrogen bonding, and it was noted that this resembled the hydrogen-bonding pattern in the mismatched base pair guanine-thymine, in which two

water molecules bridge the mispaired bases. More significantly, the molecular ribbon contains parallel strands of naphthylene residues separated by 12.42 Å, which was noted to have interesting implications for long-range energy transfer or electron transfer.

Likewise, the robustness of the guanidinium-sulfonate hydrogen-bonded sheets suggests possibilities for integrating functional molecules into two-dimensional layers. These may include networks formed from sul-

fonates containing diacetylenes, analogous to diacetylenes confined between inorganic layers of metal phosphates.⁷² The use of sulfonated dyes may lead to interesting optical materials that take advantage of the optical transparency of the guanidinium–sulfonate network. Sulfonates with ligands capable of binding to metal complexes may enable introduction of magnetic centers into the bilayer region. The reduction of the crystal engineering to a single dimension, made possible by the robust hydrogen-bonded sheet, should greatly facilitate the design of such materials.

Acknowledgment. The authors gratefully acknowledge the financial support of the National Science Foundation and the Office of Naval Research.

References

- (1) Schmidt, G. M. *J. Pure Appl. Chem.* **1971**, *27*, 647. (b) Cohen, M. D.; Schmidt, G. M. *J. Chem. Soc.* **1996**, 1964 and three following papers.
- (2) Desiraju, G. R. *Crystal Engineering: The Design of Organic Solids*; Elsevier: New York, 1989.
- (3) *Nonlinear Optical Properties of Organic Molecules and Crystals*; Chemla, D. S., Zyss, J., Eds.; Academic Press: Orlando, FL, 1987; Vol. 1.
- (4) *Extended Linear Chain Compounds*; Miller, J. S., Ed.; Plenum: New York, 1982–83; Vols. 1–3.
- (5) *Organic Superconductors*; Williams, J. M.; Ferraro, J. R.; Thorn, R. J.; Carlson, K. D.; Geiser, U.; Wang, A. H.; Kini, A. M.; Whangbo, M.-H. Prentice Hall: Englewood Cliffs, NJ, 1992.
- (6) Miller, J. S.; Epstein, A. J. *Angew. Chem., Int. Ed. Engl.* **1994**, *33*, 385.
- (7) An interesting description of polymorphism recently appeared: Dunitz, J. D.; Bernstein, J. *Acc. Chem. Res.* **1995**, *28*, 193.
- (8) Hillier, A. C.; Maxson, J. B.; Ward, M. D. *Chem. Mater.* **1994**, *6*, 2222. (b) Carter, P. W.; Ward, M. D. *J. Am. Chem. Soc.* **1994**, *116*, 769. (c) Bonafede, S.; Ward, M. D. *J. Am. Chem. Soc.* **1995**, *117*, 7853.
- (9) Wu, G.-G.; Bein, T. *Chem. Mater.* **1994**, *6*, 1109.
- (10) Wang, Y.; Herron, N. *J. Phys. Chem.* **1991**, *95*, 525. (b) Wang, Y.; Herron, N. *J. Phys. Chem.* **1989**, *92*, 4988. (c) Herron, N.; Wang, Y.; Eddy, M.; Stucky, G. D.; Cox, D. E.; Moller, K.; Bein, T. *J. Am. Chem. Soc.* **1989**, *111*, 530.
- (11) Putta, P. K.; Puri, M. *J. Phys. Chem.* **1989**, *93*, 376. (b) Hansen, H. C. B.; Taylor, R. M. *Clay Miner.* **1986**, *26*, 311.
- (12) Cao, G.; Hong, H.-G.; Mallouk, T. E. *Acc. Chem. Res.* **1992**, *25*, 420.
- (13) Thompson, M. E. *Chem. Mater.* **1994**, *6*, 1168.
- (14) Kitaigorodsky, A. I. *Organic Chemical Crystallography*; Consultants Bureau: New York, 1961.
- (15) Kitaigorodsky, A. I. *Molecular Crystals and Molecules*; Academic Press: New York, 1973.
- (16) Scaringe, R. P. In *Electron Crystallography of Organic Molecules*; Fryer, J. R., Dorset, D. L., Eds.; Kluwer: Dordrecht, 1990; p 85.
- (17) Scaringe, R. P.; Perez, S. *J. Phys. Chem.* **1987**, *91*, 2394.
- (18) Gavezotti, A. *J. Am. Chem. Soc.* **1991**, *113*, 4622.
- (19) Perlstein, J. *J. Am. Chem. Soc.* **1992**, *114*, 1955.
- (20) Perlstein, J. *J. Am. Chem. Soc.* **1994**, *116*, 455.
- (21) Perlstein, J. *J. Am. Chem. Soc.* **1994**, *116*, 11420.
- (22) Bernstein, J.; Etter, M. C.; Leiserowitz, L. In *Structure Correlation*; Dunitz, J., Burgi, H.-B., Eds.; VCH: New York, 1994.
- (23) Taylor, R.; Kennard, O. *J. Am. Chem. Soc.* **1982**, *104*, 5063.
- (24) Etter, M. C. *Acc. Chem. Res.* **1990**, *23*, 120.
- (25) Etter, M. C. *J. Am. Chem. Soc.* **1982**, *104*, 1095.
- (26) Taylor, R.; Kennard, O. *Acc. Chem. Res.* **1984**, *17*, 320.
- (27) Donahue, J. *J. Am. Chem. Soc.* **1952**, *56*, 502.
- (28) Chang, Y.-L.; West, M.-A.; Fowler, F. W.; Lauher, J. W. *J. Am. Chem. Soc.* **1993**, *115*, 5991.
- (29) Geib, S. J.; Vicent, C.; Fan, E.; Hamilton, A. D. *Angew. Chem., Int. Ed. Engl.* **1993**, *32*, 119.
- (30) Hanessian, S.; Gomtsyan, A.; Simard, M.; Roelens, S. *J. Am. Chem. Soc.* **1994**, *116*, 4495.
- (31) Ghadiri, M. R.; Kobayashi, K.; Granja, J. R.; Chadha, R. K.; McRee, D. E. *Angew. Chem., Int. Ed. Engl.* **1995**, *34*, 93.
- (32) Panunto, T. W.; Urbanczyk-Lipkowska, Z.; Johnson, R.; Etter, M. C. *J. Am. Chem. Soc.* **1987**, *109*, 7786.
- (33) Frankenbach, G. M.; Etter, M. C. *Chem. Mater.* **1992**, *4*, 272.
- (34) Leiserowitz, L. *Acta Crystallogr.* **1976**, *B32*, 775.
- (35) Etter, M. C.; Frankenbach, G. M. *Chem. Mater.* **1989**, *1*, 10.
- (36) Hosseini, M. W.; Ruppert, R.; Schaeffer, P.; De Cian, A.; Kyritsakas; Fischer, J. *J. Chem. Soc., Chem. Commun.* **1994**, 2135.
- (37) Ward, M. D.; Fagan, P. J.; Calabrese, J. C., unpublished results.
- (38) Speakman, J. C. *Struct. Bonding* **12**.
- (39) Lehn, J.-M.; Mascal, M.; DeCian, A.; Fischer, J. *J. Chem. Soc., Perkin Trans. 2* **1992**, 461.
- (40) Lehn, J.-M.; Mascal, M.; DeCian, A.; Fisher, J. *J. J. Chem. Soc., Chem. Commun.* **1990**, 479.
- (41) Zerkowski, J. A.; Seto, C. T.; Whitesides, G. M. *J. Am. Chem. Soc.* **1992**, *114*, 5473.
- (42) Zerkowski, J. A.; Whitesides, G. M. *J. Am. Chem. Soc.* **1994**, *116*, 4305.
- (43) Zerkowski, J. A.; MacDonald, J. C.; Seto, C. T.; Wierda, D. A.; Whitesides, G. M. *J. Am. Chem. Soc.* **1994**, *116*, 2832.
- (44) Hollingsworth, M. D.; Brown, M. E.; Santarsiero, B. D.; Huffman, J. C.; Goss, C. R. *Chem. Mater.* **1994**, *6*, 1227.
- (45) Duchamp, D. J.; Marsh, R. E. *Acta Crystallogr.* **1969**, *B25*, 5.
- (46) Kolotuchin, S. V.; Fenlon, E. E.; Wilson, S. R.; Loweth, C. J.; Zimmerman, S. C. *Angew. Chem., Int. Ed. Engl.* **1995**, *34*, 2654.
- (47) Seto, C. T.; Whitesides, G. M. *J. Am. Chem. Soc.* **1990**, *112*, 6409.
- (48) Copp, S. B.; Subramanian, S.; Zaworotko, M. *J. Angew. Chem., Int. Ed. Engl.* **1993**, *32*, 706.
- (49) Ung, A. T.; Bishop, R.; Craig, D. C.; Dance, I. G.; Scudder, M. L. *J. Chem. Soc., Chem. Commun.* **1993**, 322.
- (50) Venkataraman, D.; Lee, S.; Zhang, J.; Moore, J. S. *Nature* **1994**, *371*, 591.
- (51) Hart, H.; Lin, L. T. W.; Ward, D. L. *J. Am. Chem. Soc.* **1984**, *106*, 4043.
- (52) Otto, J. *Acta Crystallogr. B* **1972**, *28*, 543.
- (53) Eaton, D. F.; Anderson, A. G.; Tam, W.; Wang, Y. *J. Am. Chem. Soc.* **1987**, *109*, 1886.
- (54) Hollingsworth, M. D.; Santarsiero, B. D.; Harris, K. D. M. *Angew. Chem., Int. Ed. Engl.* **1994**, *33*, 649.
- (55) Ermer, O. *Angew. Chem., Int. Ed. Engl.* **1988**, *27*, 829.
- (56) Ermer, O. *J. Am. Chem. Soc.* **1988**, *110*, 3747.
- (57) Ermer, O.; Lindenberg, L. *Helv. Chim. Acta* **1991**, *74*, 825.
- (58) Ermer, O.; Eling, A. *J. Chem. Soc., Perkin Trans. 2* **1994**, 925.
- (59) Simard, M.; Su, D.; Wuest, J. D. *J. Am. Chem. Soc.* **1991**, *113*, 4696.
- (60) Wang, J.; Simard, M.; Wuest, J. D. *J. Am. Chem. Soc.* **1994**, *116*, 12119.
- (61) Copp, S. B.; Subramanian, S.; Zaworotko, M. *J. J. Chem. Soc., Chem. Commun.* **1993**, 1078.
- (62) Copp, S. B.; Subramanian, S.; Zaworotko, M. *J. J. Am. Chem. Soc.* **1992**, *114*, 8719.
- (63) Zaworotko, M. *J. Chem. Soc. Rev.* **1994**, 283.
- (64) Gardner, G. B.; Venkataraman, D.; Moore, J. S.; Lee, S. *Nature* **1995**, *374*, 792.
- (65) Hoskins, B. F.; Robson, R. *J. Am. Chem. Soc.* **1990**, *112*, 1546.
- (66) Goodgame, D. M. L.; Menzer, S.; Smith, A. M.; Williams, D. J. *Angew. Chem., Int. Ed. Engl.* **1995**, *34*, 574.
- (67) Russell, V. A.; Etter, M. C.; Ward, M. D. *J. Am. Chem. Soc.* **1994**, *116*, 1941.
- (68) Russell, V. A.; Etter, M. C.; Ward, M. D. *Chem. Mater.* **1994**, *6*, 1206.
- (69) Cai, H.; Hillier, A. C.; Franklin, K.; Nunn, C. C.; Ward, M. D. *Science* **1994**, *266*, 1551.
- (70) Russell, V. A.; Ward, M. D., to be submitted. (b) Russell, V. A. Ph.D. Thesis, University of Minnesota.
- (71) Russell, V. A.; Li, W.; Ward, M. D., to be submitted.
- (72) Cao, G.; Mallouk, T. E. *J. Sol. State Chem.* **1991**, *94*, 59.

CM9600743